JCHR (2024) 14(4), 727-740

Journal of Chemical Health Risks

sanad.iau.ir/journal/jchr

ORIGINAL ARTICLE

Kinetic, Isotherm, and Thermodynamic Modeling of Methylene Blue Adsorption by Hibiscus Plant Waste Derived Biosorbents

Khaled Muftah Elsherif [*1,2], Abdulfattah Mohamed Alkherraz [3], Aisha Hussein Madri[3], Abdelmeneim El-Dali[1], Maysson Mohammed Yaghi[4]

[1]*Libyan Authority for Scientific Research, Tripoli, Libya*

[2]*Chemistry Department, Faculty of Science, University of Benghazi, Benghazi, Libya*

[3]*Chemistry Department, Faculty of Science, Misurata University, Misurata, Libya*

[4]*Department of Chemistry, Faculty of Science Al-Abyar, University of Benghazi, Benghazi, Libya*

Received: 8 February 2024 *Accepted: 22 June 2024*

KEYWORDS

Methylene blue,
Biosorption,
Isotherms,
Kinetics,
Thermodynamics

ABSTRACT: Dye pollution is a severe environmental issue for which there are no short-term fixes. Adsorption has become the most popular method for removing dyes because of its remarkable effectiveness, ease of use, affordability, and environmental friendliness. This study intends to assess how well two biosorbents; dried powder (DHM) and charcoal (CHM), made from hibiscus plant debris remove methylene blue (MB) from aqueous solutions. Adsorption kinetics, isotherms, and thermodynamics were examined in order to better understand the adsorption mechanisms. The adsorption capacity and efficiency of methylene blue on both adsorbent materials were assessed using the batch adsorption experiment. Several parameters, including pH, initial dye concentration, contact time, adsorbent dosage, and temperature, were examined in relation to the biosorption process. For both biosorbents, the biosorption equilibrium was reached in 20 min, and at pH 10.5, the maximum adsorption capacities were 11.60 and 11.80 mg g^{-1} for DHM and CHM, respectively. Despite not going through the extra activation step, CHM was assessed in its non-activated condition and, surprisingly, showed equal or even slightly superior MB adsorption ability than DHM. The experimental data was well-fitted by the Freundlich and pseudo-second-order models, indicating a physical adsorption mechanism. The thermodynamic study's conclusions demonstrated that MB's adsorption on CHM was non-spontaneous and endothermic, with positive values for ΔH^o (15.900 kJ mol^{-1}), ΔG^o (0.404 kJ mol^{-1}), and ΔS^o (0.052 kJ mol^{-1} K^{-1}). The MB adsorption on DHM, on the other hand, was exothermic and spontaneous, with negative values for ΔG^o (-5.41 kJ mol^{-1}), ΔH^o (-42.36 kJ mol^{-1}), and ΔS^o (-0.124 kJ mol^{-1} K^{-1}). The study's findings demonstrate that hibiscus plant waste can be utilised as an inexpensive, environmentally beneficial biosorbent to remove MB from wastewater.

INTRODUCTION

The effective management of water resources in a sustainable and integrated manner presents a significant and complex challenge for numerous nations. Within the realm of sustainable water management, the treatment of wastewater has a vital function in ensuring the overall quality of water. However, the contamination of water sources, both natural and industrial, by various pollutants, particularly dyes, has emerged as a pressing

*Corresponding author: elsherif27@yahoo.com (Kh. Muftah Elsherif)
DOI: 10.60829/jchr.2024.1977

environmental and health concern, posing risks to both society and ecosystems [1-4].

The presence of high concentrations of dyes in water sources and industrial wastewater streams has become a critical issue many countries face. These dyes are known for their persistence, high toxicity, and carcinogenic impurities. Furthermore, they have the potential to bioaccumulate within the food chain, ultimately affecting human health. Recent studies have highlighted the detection of numerous harmful chemicals in drinking water at alarming levels across different regions worldwide. Among the most prevalent toxic pollutants are the harmful chemicals and dyes in wastewater generated by heavy industries and various human activities, necessitating their treatment before discharge into the environment [5-10].

Industries worldwide, including the cosmetic, food, and paper sectors, heavily rely on dyes. Among these industries, the textile sector is the primary consumer of dyes due to their favorable attributes, such as chemical stability and ease of synthesis. The global production of dyes surpasses 7 × 105 tons annually, with Azo coloration constituting 60 to 70% of the total output. However, the widespread use of these synthetic dyes gives rise to significant environmental concerns [11-13]. The aqueous effluents generated by these industries often contain tinted wastewater, which can harbor chemicals that pose a threat to microbial populations and possess toxic or carcinogenic properties for humans and animals. These environmental issues stem from using synthetic dyes, necessitating exploring alternative approaches to mitigate their negative impact [12].

Methylene blue (MB), an extensively employed cationic dye with the chemical formula C16H18ClN3S, finds wide application as a chemical indicator, dye, and biological stain. The printing and dyeing industries generate substantial wastewater containing organic dyes. This dye wastewater exhibits distinct characteristics, including significant discharge, intense chromaticity, high concentration of organic matter, and limited biodegradability. Consequently, it significantly impacts the overall health of water bodies and hampers the photosynthesis process of microorganisms within the aquatic environment [14, 15].

As a result, before releasing the wastewater into bodies of water, the aforementioned enterprises must put in place wastewater treatment systems. Currently, a wide range of techniques are used to treat wastewater, such as adsorption, advanced oxidation, coagulation, flocculation, and photocatalysis. While there are benefits and drawbacks to each strategy, the main issue with the majority of these technologies is their high cost and possibility for secondary pollution. Adopting a water treatment technique that can overcome the shortcomings of current technologies is therefore essential [16–23].

Adsorption has become the most popular method for treating wastewater because of its remarkable performance, ease of use, affordability, and environmental friendliness. Adsorption is an advantageous option for water treatment since it can be used to overcome the shortcomings of other treatment technologies [24–27]. Many biomaterials have been studied for their potential in adsorbing methylene blue. These materials include silica, zeolites, alumina, activated carbon derived from fruit waste, agro-industrial wastes, composite hydrogels based on polysaccharides, activated carbon obtained from eucalyptus residue treated with phosphoric acid, chemically modified lychee seed biochar, transition metal oxides, and various other biomaterials. These biomaterials have undergone extensive investigation for their effectiveness in methylene blue adsorption [28-40].

The purpose of this work is to employ the dried powder and charcoal surfaces that are obtained from the waste of hibiscus plants as very effective biosorbents for the removal of methylene blue (MB) from aqueous solutions. Additionally, by examining adsorption kinetics, isotherms, and thermodynamics, the adsorption mechanisms were examined. This study advances the use of the underutilised byproduct of hibiscus plants as a useful biosorbent for dye-contaminated water treatment. The potential of hibiscus plant waste as a biosorbent has not yet been investigated in previous research.

MATERIALS AND METHODS

Chemicals

All the chemicals utilised in this study were of analytical quality and were not subjected to any purifying procedures. The experiment employed methylene blue

indicator ($C_{16}H_{18}ClN_3S$) with a purity level of ≥98.5%. Merck provided various reagents along with analytical reagent (AR) grade sodium hydroxide (NaOH) and hydrochloric acid (HCl). For the experiment, deionized (DI) water was procured from a Millipore-Q system.

Analysis of Dye Concentrations

Methylene blue (MB) was first dissolved in deionized water to provide an initial stock solution with a concentration of 500 mg L^{-1}. To achieve concentrations of 1 to 200 mg L^{-1}, this stock solution was diluted later. To alter the pH of the suspension containing the adsorbents, either 0.1 M aqueous solutions of NaOH or HCl were used. A pH metre made in the United Kingdom, the Jenway 3305, was used to measure the pH values. To quantify MB at a temperature of 25°C, calibration curves in the range of 1.0–10 mg L^{-1} were created. A UV-visible spectrophotometer (JENWAY 6305 Spectrophotometer) was used to measure the concentrations of MB both before and after adsorption. Filter paper No. 1 from Whatman was used to filter the samples.

Preparation of Adsorbent Materials

The waste from hibiscus plants used in this study came from a nearby Libyan farm in Misurata. This waste material led to the development of two different adsorbents. In order to get ready for the dry hibiscus material (DHM), the plant was thoroughly cleaned and then washed with double distilled water to remove any unnecessary particles from its exterior. It was then dried in the sun and baked for around 24 hours at 70°C in a hot air oven. The hulls were dried, then processed with an electric grinder and filtered to produce particles smaller than 125 μm. For later experimental use, the resultant substance was kept apart in special containers [41].

The dried hibiscus material was pyrolyzed in a furnace for two hours at 550°C in order to produce the charcoal hibiscus material (CHM). The resultant biochar was removed and subjected to additional processing following the pyrolysis process. After being ground into a fine powder and sifted to get the right particle size, double distilled water was used to wash it. To guarantee its dryness, the biochar was lastly dried at 60°C [42, 43].

Adsorption Experiments

The purpose of the batch adsorption experiment was to assess the capacity and adsorption effectiveness of methylene blue on both adsorbent materials. The study examined a range of experimental factors, such as pH (between 3 and 10), starting dye concentration (between 5.0 and 200.0 mg L^{-1}), contact duration (between 0.0 and 30.0 min), adsorbent dosage (between 0.1 and 1.0 g), and temperature (between 298, 303, 308, 313, 318, and 323 K) [44].

A pH metre was used to measure the pH of the solution after it had been initially adjusted with either 0.1 M hydrochloric acid (HCl) or sodium hydroxide (NaOH) solution. A 150 mL conical flask holding 50 mL of the methylene blue solution was filled with a precise amount of adsorbent material at different concentrations. Every mixture was stirred for the specified durations of time at a rate of 175 revolutions per minute (rpm) at 25°C. The samples were filtered and examined after the adsorption procedure. Each experiment was conducted thrice to ensure repeatability [45].

Using the following formulas [46, 47], the equilibrium amount of methylene blue adsorbed (Q_e) in milligrams per grams (mg g^{-1}) and the percentage of methylene blue adsorbed (%R) were determined:

$$Q_e = \frac{(C_o - C_e) x\ V}{M} \qquad (1)$$

$$\%R = \frac{(C_o - C_e)}{C_o} \times 100 \qquad (2)$$

where the initial safranin concentration, equilibrium safranin concentration, volume of aqueous media, and mass of the dry adsorbent are represented by C_o (mg L^{-1}), C_e (mg L^{-1}), V (L), and M (g), respectively.

Adsorption Kinetics

Equations 3 and 4, which represent the pseudo-first order and pseudo-second order kinetic models, respectively, were used to evaluate the kinetic properties of MB dye removal utilising the DHM and CHM biosorbents [48, 49]:

$$\mathrm{Log}(Q_e - Q_t) = \mathrm{Log}Q_e - k_1 t \qquad (3)$$

$$\frac{t}{Q_t} = \frac{1}{k_2 Q_e^2} + \frac{1}{Q_e}\ t \qquad (4)$$

The amount of substance adsorbed is represented by the

equilibrium sorption capacity (Q_e) and the sorption capacity at a particular time (Q_t). Pseudo-first order sorption rate constant is k_1, and pseudo-second order sorption rate constant is k_2, both expressed in grams per milligrams per minute.

Adsorption Isotherms

The adsorption efficiency of most adsorption processes heavily relies on the adsorbents' capacity to adsorb various components within a mixture. Hence, it is crucial to develop a comprehensive understanding of the properties governing the equilibrium between the adsorbent and adsorbate [11]. The two-parameter equation-based Langmuir and Freundlich models are widely used in scientific literature to describe the non-linear equilibrium between the adsorbed pollutant (Q_e) and the residual pollutant in solution (C_e) when the reaction is carried out at a constant temperature [50]. To evaluate the suitability of these classical models and verify the outcomes, the linear forms of these models were used. The following linear equations [51, 52] represent the models:

$$\frac{C_e}{Q_e} = \frac{1}{b\,Q_m} + \frac{C_e}{Q_m} \qquad (5)$$

$$\mathrm{Log}Q_e = \mathrm{Log}K_f + \frac{1}{n}\,\mathrm{Log}C_e \qquad (6)$$

The Langmuir model in Equation (5) includes parameters Q_m, b, and C_e, which stand for the maximal adsorption capacity, Langmuir constant, and equilibrium dye concentration, respectively. The Freundlich equation (6) involves the heterogeneity factor 1/n, where n (g L^{-1}) represents the degree of adsorption deviance from linearity, and the Freundlich constant K_f, which is related to bonding energy. Furthermore, the following relationship can be used to find the Langmuir model parameter R_L:

$$R_L = \frac{1}{1+b\,C_o} \qquad (7)$$

The parameter for dimensionless equilibrium R_L is closely related to the Langmuir model, where C_o and b stand for the equilibrium dye concentrations and Langmuir constant, respectively. Adsorption type is determined by the R_L value: $R_L = 0$ indicates irreversible adsorption, $0 < R_L < 1$ indicates favourable adsorption, and $R_L > 1$ indicates unfavourable adsorption [6]. The degree to which the relationship between solution concentration and adsorption is non-linear is indicated by the n value: adsorption exhibits a linear pattern when n = 1, a chemical process when n < 1, and a physical process when n > 1 [8].

To validate the results, the Temkin and Dubinin-Kaganer-Radushkevich (D-R) adsorption isotherm models were also used. The Temkin model's linear form, represented by equation (8), takes into consideration the consequences of any indirect interactions that may have occurred during the adsorption process between the adsorbent and adsorbate. As the adsorbed molecular layer gets saturated, this isotherm predicts a linear decrease in the heat of adsorption for all molecules [23].

$$Q_e = B_T\ \ln K_T + B_T\ \ln C_e \qquad (8)$$

Included in the equation are the Temkin isotherm constant (KT, L mg^{-1}) and the Temkin adsorption constant (BT, J mol^{-1}).

When describing the adsorption mechanism on non-uniform surfaces with a Gaussian energy distribution, the Dubinin-Radushkevich adsorption isotherm technique is frequently employed. The Dubinin-Radushkevich isotherm does not require a homogenous surface or constant adsorption potentials, in contrast to other isotherm models. Alternatively, the apparent energy of adsorption can be approximated. The linearized form of the Dubinin-Radushkevich isotherm is represented by equation [10]:

$$\log Q_e = \log Q_m - \beta\,\varepsilon^2 \qquad \mathbf{(9)}$$

Where ε (J mol^{-1}) is the Polanyi potential, a measurement of the potential energy of adsorption per mole of adsorbate, and β ($mol^2.J^{-2}$) is the Dubinin-Radushkevich constant, which is related to the characteristic energy of adsorption.

Thermodynamics Investigation

An essential component of the study of adsorption studies is thermodynamics. The following equations [10, 51, and 53] can be used to express the thermodynamic characteristics that determine the process's spontaneity and thermodynamic feasibility: entropy change (ΔS^o),

enthalpy change (ΔH^o), and Gibbs free energy (ΔG^o):

$$\Delta G = \Delta H - T\,\Delta S \qquad (10)$$

$$\Delta G = -RT\,\mathrm{Ln}\,K_c \qquad (11)$$

The standard thermodynamic equilibrium constant should be calculated using activity rather than concentration in order to determine the apparent equilibrium constant of adsorption (K_c):

$$K_d = \frac{Q_e}{C_e} \qquad (12)$$

Equation (13) establishes the relationship between entropy, enthalpy, and Kc as illustrated below:

$$\mathrm{Ln}K_d = \frac{\Delta S}{R} - \frac{\Delta H}{RT} \qquad (13)$$

RESULTS AND DISCUSSION

Effect of Contact Time

Because the length of contact time is critical to the removal of MB dye, its impact was examined in multiple batches over the course of 0 to 30 minutes. Both of the adsorbent surfaces' obtained results are shown in Figures 1a and 1b. Interestingly, the adsorption process proceeded quickly in 15 min and was slowly getting closer to equilibrium in 20 min. The high surface area and porous structure of DHM and CHM, which promote effective MB molecule contact and diffusion, may be responsible for this quick initial adsorption. Additionally, favourable electrostatic interactions between the adsorbent surfaces and MB might play a role in the fast initial uptake. The maximum adsorption capacities were observed to be 11.40 mg g^{-1} and 11.60 mg g^{-1} at the 20-min mark for DHM and CHM, correspondingly. Subsequently, a saturation point was reached, indicating the attainment of adsorption process equilibrium. [7]

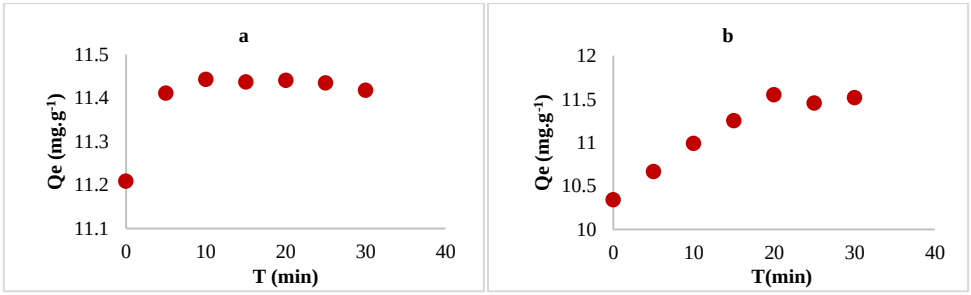

Figure 1. Effect of contact time on MB adsorption onto: a) DHM, b) CHM.

The pseudo-first-order (PFO) fit was used to analyse the experimental data in order to ascertain the mechanism of the adsorption process, and the evaluation of adsorption kinetic parameters was made possible by pseudo-second-order (PSO) kinetic models [47]. In the case of the PFO model, there was a noticeable deviation from linearity in the linear fitting, and a significant disparity between the calculated and experimental adsorption capacities was observed (see Figures 2a and 2b).

Conversely, the PSO model exhibited excellent linear fitting [Figures 2c and 2d], with no deviation observed between the experimental (11.40 and 11.60 mg g^{-1}) and calculated Q_e (11.43 and 11.60 mg g^{-1}). Table 1 displays the kinetic parameters. Previous investigations have reported similar observations [7-11].

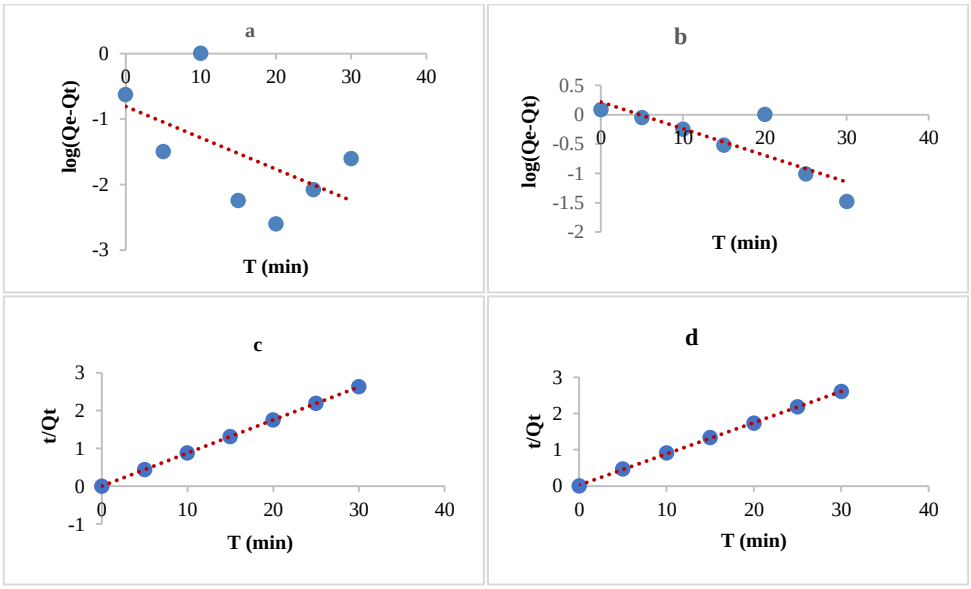

Figure 2. Kinetic study of MB adsorption: a) PFO for DHM, b) PFO for CHM, c) PSO for DHM, d) PSO for CHM

Table 1. Kinetic parameters of MB dye onto DHM and CHM.

First order	**Q_e (calculated) (mg g^{-1})**	**Q_e (experimentally) (mg g^{-1})**	***k_1*** **(min^{-1})**	**R^2**
DHM	0.156	11.40	٠.٠478	0.312
CHC	1.652	11.60	٠.٠454	0.698
Second order	Q_e (calculated) (mg g^{-1})	Q_e (experimentally) (mg g^{-1})	k_2 (g.mg^{-1} min^{-1})	R^2
DHM	11.43	11.40	0.708	1.000
CHC	11.60	11.60	4.080	1.000

Effect of Adsorbent Dose

For a given initial concentration of the adsorbate, the amount of adsorbent used is a critical factor in determining the sorption capacity [14]. The adsorption capacity of MB dye on both surfaces as a function of DHM and CHM dose (varying from 0.1 to 1.0 g) is depicted in Figures 3a and 3b. Adsorption effectiveness for dye removal increases with an increase in the adsorbent dosage. This pattern can be explained by a larger dose of adsorbent, which produces more accessible adsorption sites and increases the amount of dye that is adsorbed. However, partial adsorption site saturation is responsible for the decline in adsorption capability with increasing adsorbent dosage [54]. Another possibility is that a higher adsorbent dose promotes inter-particle interactions, such as aggregation, which reduces the adsorbent's overall surface area and increases the diffusional path length [41].

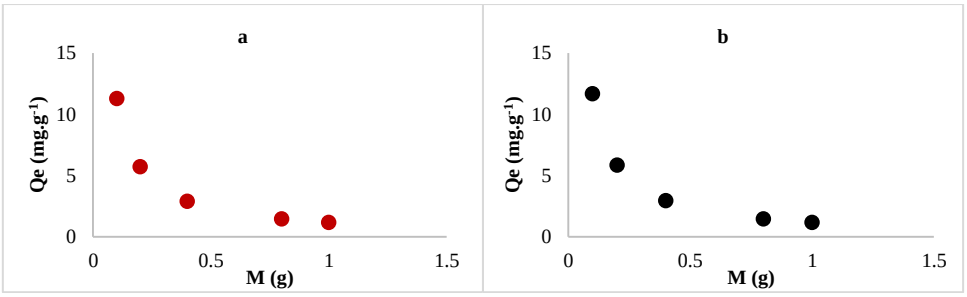

Figure 3. Effect of adsorbent dose on MB adsorption onto: a) DHM, b) CHM.

Effect of pH

A significant factor that was studied was the effect of pH on the adsorption process; the results of the experiments are shown in Figures 4a and 4b. Higher initial pH levels are associated with an increase in the adsorbent's adsorption capability. In particular, the adsorption capacity for DHM and CHM reached 11.60 and 11.80 mg g^{-1}, respectively, at an initial pH of 10.5. Theoretically, an important adsorption force in the pH range of 3.2-11 is the electrostatic adsorption between the cationic methylene blue and the adsorbent. To further improve adsorption, the adsorbent also has a comparatively large surface negative charge potential energy (when the initial pH exceeds pH_{pzc}, the pH at which the net electrical charge on an adsorbent's surface becomes zero).

On the other hand, ion exchange and hydrogen bonding are the main mechanisms for adsorption when the pH is lower than pH_{pzc} [54]. Based on an analysis of the adsorbent's zero charge point (pH_{pzc}), which was found to be 3.2, Tang et al. [9] postulated an adsorption mechanism. They suggest that the adsorbent surface is positively charged at pH values less than 3.2 and negatively charged at pH values more than 3.2. Additionally, as the pH of the solution rises, the adsorbent surface displays a greater negative potential energy [20, 22]. It is anticipated that at pH 11, adsorbents such as DHM and CHM will have a greater ability to adsorb cationic dyes.

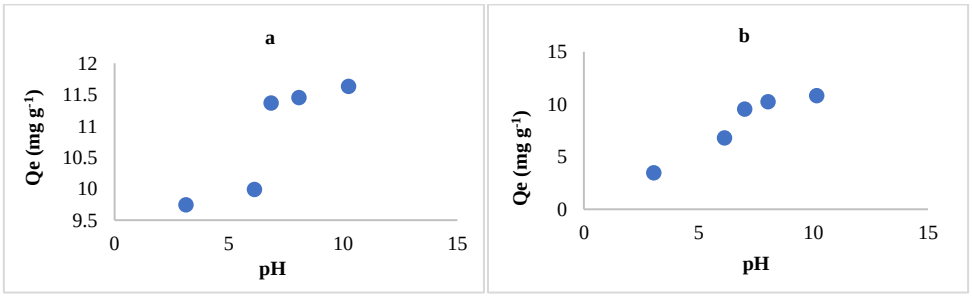

Figure 4. Effect of pH on MB adsorption onto: a) DHM, b) CHM.

Effect of Initial Dye Concentration

The process of dye adsorption involves the buildup of dye at the interface between the liquid and solid phases. As shown in Figures 5a and 5b, this phenomena was investigated by looking at the effect of initial dye concentration while holding other parameters constant. A progressive increase in the amount of dye adsorbed was seen at higher starting concentrations. This is explained by the fact that the initial concentration of the dye acts as a catalyst to push past the resistance that arises when the dye is mass transferred between the aqueous and solid phases [39]. Furthermore, increasing the initial dye concentration enhances the bond between the dye molecules and the adsorbent substance [56]. Consequently, elevating the initial concentration of MB dyes amplifies their uptake during adsorption, as depicted in Figures 5a and 5b.

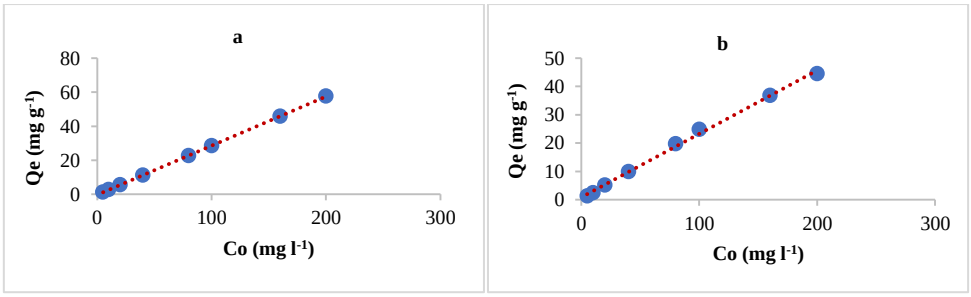

Figure 5. Effect of initial concentration on MB adsorption onto: a) DHM, b) CHM.

Analysis of adsorption isotherms, which offers insightful information for optimisation, greatly aids in the characterization of adsorption systems. The maximum adsorption capacity may be calculated thanks to these isotherms, which clarify the equilibrium relationship between the adsorbent and adsorbate [41, 44]. As shown in Figures 6a through 6h, the adsorption isotherms of MB dye on DHM and CHM were assessed in this work using the Langmuir, Freundlich, Temkin, and Dubinin-Radushkevich models.

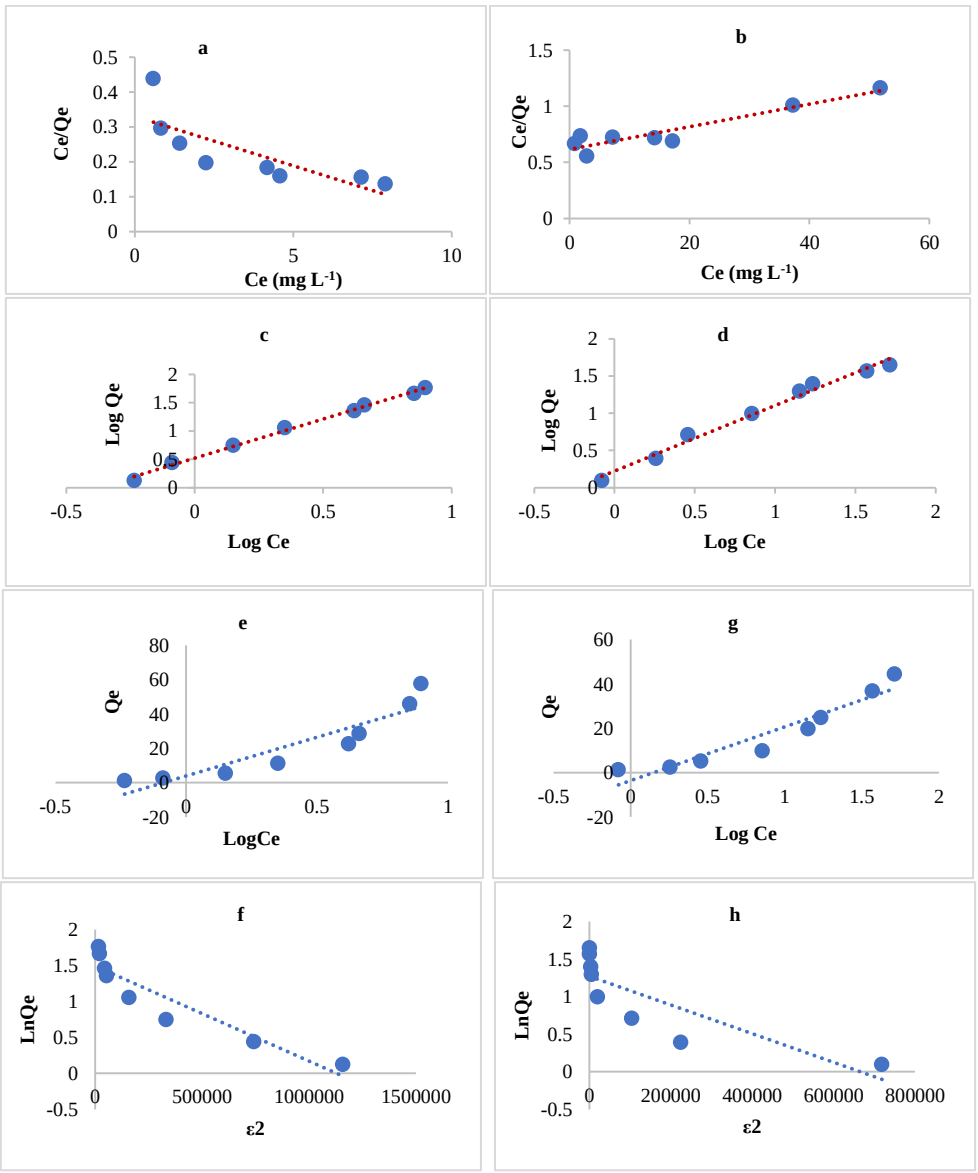

Figure 6. Langmuir (a & b), Freundlich (c & d), Temkin (e & g), and D-R (f & h) adsorption isotherm plots of MB dye adsorption onto DHM & CHM

The correlation coefficients associated with the Freundlich isotherm (0.995 and 0.985) clearly exceeded

those of the Langmuir isotherm (0.632 and 0.879), Temkin (0.8482 and 0.9059), and D-R (0.8756 and 0.6980), as evidenced by the results displayed in Figures 6a, 6b, 6c, 6d, 6e, 6f, 6g, 6h, and Table 2. This disparity implies that the adsorbent's surface was heterogeneous and that the adsorption system contained multilayer adsorption sites. Furthermore, the computed value of n (n>1) shows that physical processes account for the majority of the adsorption process. The dimensionless constant R_L, which ranges from 0.055 to 0.238, is found to be within the desirable range according to the Langmuir parameters. Maximum adsorption capacities (in mg g^{-1}) of 35.34 for DHM and 99.01 for CHM were obtained from the Langmuir expression. These values, however, did not agree with the outcomes of the experiment.

Table 2. Parameter values of the isotherm models in the adsorption of MB onto DHM & CHM

Langmuir	**Q_m (mg g^{-1})**	**Q_m Experimental (mg g^{-1})**	**b (L mg^{-1})**	**R_L**	**R^2**
DHM	35.34	44.46	0.086	0.055	0.632
CHM	99.01	57.63	0.016	0.238	0.879
Freundlich	K_f ((mg g^{-1})(mg L^{-1})$^{1/n}$)		n (g L^{-1})		R^2
DHM	3.30		1.00		0.995
CHM	1.67		1.13		0.985
Temkin	B_T (J mol^{-1})		K_T (L mg^{-1})		R^2
DHM	45.1		1.09		0.8482
CHM	24.3		1.16		0.9059
D-R	Q_m (mg g^{-1})		β (mol² J^{-2})		R^2
DHM	1×10^{-6}		4.44		0.8756
CHM	2×10^{-6}		3.56		0.6980

Effect of Temperature and Thermodynamics

At various temperature values (298, 303, 308, 313, 318, and 323 K), the impact of temperature on MB adsorption was examined; the findings are shown in Figures 7a and 7b. The ability of MB to adsorb on CHM was shown to increase with temperature, suggesting that the adsorption process was endothermic spontaneously. On the other hand, it was discovered that when the temperature was raised, MB's capacity for adsorption on DHM reduced, indicating an exothermic adsorption process that occurred naturally.

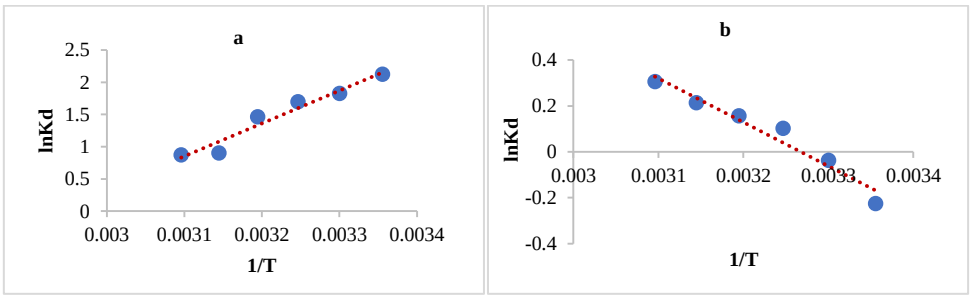

Figure 7. Van't Hoff plot of the adsorption of MB dye onto: a) DHM, b) CHM.

The higher mobility of adsorbate molecules within the interior pores and outside border layer of the solid adsorbent particle may be responsible for the endothermic event. More adsorbate molecules accumulate sufficient energy to interact with the binding sites on the particle's surface as the number of adsorbate

molecules rises [57]. Upon computation, the thermodynamic properties of MB adsorption onto CHM are shown in Table 3. The computed values of ΔG^o equal 0.404 kJ mol^{-1}. The process is not viable under these conditions, as indicated by the positive value. Furthermore, a higher degree of randomness among dye molecules on the surface of the adsorbent particle than in the dye solution is indicated by the positive ΔS^o value (0.052 kJ mol^{-1} K^{-1}), which encourages solid-liquid interactions. Additionally, the observed increase in Q_e values with increased temperatures [29] and the positive ΔH^o value (15.900 kJ mol^{-1}) support the endothermic nature of the investigated adsorption process.

On the other hand, the spontaneous and thermodynamically possible adsorption of MB onto DHM is shown by the negative ΔG^o value. Generally speaking, ΔG^o values for chemisorption vary from -80 to -400 kJ mol^{-1}, while those for physisorption are found between -20 and 0 kJ mol^{-1} [58]. The ΔG^o value in this investigation was found to be -5.41 kJ mol^{-1}, suggesting that the adsorption is unusually more similar to physisorption. The process's exothermic character is confirmed by the negative value of ΔH^o (-42.36 kJ mol^{-1}). This adsorption energy is being compared to a number of forces, including coordination exchange (about 40 kJ mol^{-1}), hydrophobic bond forces (about 5 kJ mol^{-1}), van der Waals forces (4–10 kJ mol^{-1}), and chemical bond forces (>60 kJ mol^{-1}). The value of ΔH^o indicates that van der Waals and hydrophobic interactions may also be involved in the adsorption process, in addition to electrostatic attraction. Finally, a decrease in randomness at the adsorbate-solution interface during adsorption is shown by a negative value of ΔS^o. [59].

Table 3. Thermodynamic parameters for adsorption of MB onto DHM and CHM

Adsorbent	ΔG^o (kJ mol^{-1})	ΔH^o (kJ mol^{-1})	ΔS^o (kJ $mol^{-1}k^{-1}$)	R^2
DHM	-5.41	- 42.360	- 0.124	0.9522
CHM	0.404	15.900	0.052	0.9498

CONCLUSIONS

In this study, methylene blue (MB) was extracted from aqueous solutions using two biosorbents made from the waste of hibiscus plants: dried powder (DHM) and charcoal (CHM). Adsorption was affected by a number of factors, including temperature, pH, starting dye concentration, contact time, and adsorbent dosage. The physical basis of the process was disclosed by the adsorption kinetics and isotherms, which were consistent with the Freundlich and pseudo-second order models. Thermodynamic research revealed that the MB adsorption onto CHM was endothermic and non-spontaneous, whereas the adsorption onto DHM was exothermic and spontaneous. The outcomes showed that the waste from hibiscus plants can be utilised as an inexpensive and environmentally beneficial biosorbent to remove dye from wastewater. This study contributes to using underexplored plant waste as a valuable resource for environmental remediation.

ACKNOWLEDGEMENTS

We would like to express our sincere gratitude and appreciation to the Chemistry Department, Faculty of Science, Misurata University, for their invaluable support throughout this research endeavor. Their resources, facilities, and guidance were instrumental in the successful completion of this study. We are grateful for the opportunity to conduct this research within their esteemed institution

Conflict of interest

We hereby declare that there are no conflicts of interest to disclose regarding the research presented in this manuscript. All authors have no personal or financial relationships that could influence the interpretation or presentation of the data. This absence of conflicts of interest ensures the integrity and unbiased nature of our research findings and supports the transparency and credibility of this submission

REFERENCES

1. Nizam N.U.M., Hanafiah M.M., Mahmoudi E., Halim A.A., Mohammad A.W., 2021. The Removal

of Anionic and Cationic Dyes from an Aqueous Solution Using Biomass-Based Activated Carbon. Sci Rep. 11(1), 8623. https://doi.org/10.1038/s41598-021-88084-z.

2. El Hashani A., Ben Khayal N., Elsherif K.M., 2018. Selective Transport of Aromatic Compounds across Parchment Supported Prussian blue Membrane. Chem. Methodol. 2(3), 194–203. https://doi.org/10.22034/chemm.2018.60860.

3. Elsherif K.M., El-Hashani A., El-Dali A., 2013. Potentiometric Determination of Fixed Charge Density and Permselectivity for Thallium Chromate Membrane. Ann Chem Forsch. 1(3), 15–25.

4. Alkherraz A.M., Elsherif K.M., El-Dali A., Blayblo N.A., Sasi M., 2022. Thermodynamic, Equilibrium, and Kinetic Studies of Safranin Adsorption onto Carpobrotus Edulis. Asian J Nanosci Mater. 5(2), 118–131. https://doi.org/10.26655/ajnanomat.2022.2.4.

5. Elsherif K.M., El-Hashani A., El-Dali A., El-kailany R., 2014. Bi-Ionic Potential Studies for Thallium Chromate Parchment-Supported Membrane. Int J Res Pharm Chem. 4(2), 267–273.

6. Sahu S., Pahi S., Tripathy S., Singha S.K., Behera A., Sahu U.K., Patel R.K., 2020. Adsorption of Methylene Blue on Chemically Modified Lychee Seed Biochar: Dynamic, Equilibrium, and Thermodynamic Study. J Mol Liq. 315, 113743. https://doi.org/10.1016/j.molliq.2020.113743.

7. Elsherif K.M., El-Dali A., Alkarewi A.A., Ewlad-Ahmed A.M., Treban A. 2021. Adsorption of Crystal Violet Dye onto Olive Leaves Powder: Equilibrium and Kinetic Studies. Chem Int. 7(2), 79–89. https://doi.org/10.5281/zenodo.4441851.

8. Tang X., Ran G., Li J., Zhang Z., Xiang C., 2021. Extremely Efficient and Rapidly Adsorb Methylene Blue Using Porous Adsorbent Prepared from Waste Paper: Kinetics and Equilibrium Studies. J Hazard Mater. 402, 123579. https://doi.org/ 10.1016/j. jhazmat.2020.123579.

9. Elsherif K.M., El-Hashani A., El-Dali A., Saad M., 2014. Ion-Permeation Rate of (1:1) Electrolytes across Parchment-Supported Silver Chloride Membrane. Int J Chem Pharm Sci. 2 (6), 890–897.

10. Alkherraz A.M., Elsherif K.M., Blayblo N.A., 2023. Safranin Adsorption onto Acasia Plant Derived Activated Carbon: Isotherms, Thermodynamics and Kinetic Studies. Chem Int. 9(4), 134–145. https://doi.org/10.5281/zenodo.8127687.

11. Djama C., Bouguettoucha A., Chebli D., Amrane A., Tahraoui H., Zhang J., Mouni L., 2023. Experimental and Theoretical Study of Methylene Blue Adsorption on a New Raw Material, Cynara Scolymus—A Statistical Physics Assessment. Sustainability. 15(13), 10364. https://doi.org/ 10.3390/su151310364.

12. Bouguettoucha A., Chebli D., Mekhalef T., Noui A., Amrane A., 2015. The Use of a Forest Waste Biomass, Cone of Pinus Brutia for the Removal of an Anionic Azo Dye Congo Red from Aqueous Medium. Desalin. Water Treat. 55(7), 1956–1965. https://doi.org/10.1080/19443994.2014.928235.

13. Elsherif K.M., El-Hashani A., El-Dali A., Musa M., 2014. Ion Selectivity across Parchment-Supported Silver Chloride Membrane in Contact with Multi-Valent Electrolytes. Int J Anal Bioanal Chem. 4(2), 58–62.

14. Kuang Y., Zhang X., Zhou S., 2020. Adsorption of Methylene Blue in Water onto Activated Carbon by Surfactant Modification. Water. 12(2), 587. https://doi.org/10.3390/w12020587.

15. Tan I.A.W., Ahmad A.L., Hameed B.H., 2008. Adsorption of Basic Dye on High-Surface Area Activated Carbon Prepared from Coconut Husk: Equilibrium, Kinetic and Thermodynamic Studies. J Hazard Mater. 154, 337–346. https://doi.org/10.1016/j.jhazmat.2007.10.031.

16. Zaidi Z., Manchanda A., Sharma A., Shehnaz, Choudhry A., Sajid M., Khan S.A., Khan A., Chaudhry S.A., 2023. Adsorptive Removal of Methylene Blue Using Fruit Waste Activated Carbon and Its Binary Metal Oxide Nanocomposite. Chem Eng J Adv. 16, 100571. https://doi.org/ 10.1016/j.ceja.2023.100571.

17. Elsherif K.M., El-Hashani A., El-Dali A., El-kailany R., 2014. Bi-Ionic Potential Studies for Silver Thiosulphate Parchment-Supported Membrane. Int. J. Adv. Sci. Tech. Res. 1 (4), 638–646.

18. Sharma A., Mangla D., Choudhry A., Sajid M.,

Chaudhry S.A., 2022. Facile Synthesis, Physico-Chemical Studies of Ocimum Sanctum Magnetic Nanocomposite and Its Adsorptive Application against Methylene Blue. J Mol Liq. 362, 119752. https://doi.org/10.1016/j.molliq.2022.119752.

19. Alkherraz A.M., Ali A.K., Elsherif K.M., 2020. Removal of Pb(II), Zn(II), Cu(II) and Cd(II) from Aqueous Solutions by Adsorption onto Olive Branches Activated Carbon: Equilibrium and Thermodynamic Studies. Chem Int. 6(1), 11–20. https://doi.org/10.5281/zenodo.2579465.

20. Han Q., Wang J., Goodman B.A., Xie J., Liu Z., 2020. High Adsorption of Methylene Blue by Activated Carbon Prepared from Phosphoric Acid Treated Eucalyptus Residue. Powder Technol. 366, 239–248.
https://doi.org/10.1016/j.powtec.2020.02.013.

21. Alkherraz A.M., Ali A.K., Elsherif K.M., 2020. Equilibrium and Thermodynamic Studies of Pb(II), Zn(II), Cu(II) and Cd(II) Adsorption onto Mesembryanthemum Activated Carbon. J Med Chem Sci. 3 (1), 1–10. https://doi.org/ 10.33945/SAMI/JMCS.2020.1.1.

22. Sivakumar R., Lee N.Y., 2022. Adsorptive Removal of Organic Pollutant Methylene Blue Using Polysaccharide-Based Composite Hydrogels. Chemosphere. 286, 131890. https://doi.org/10.1016/j.chemosphere.2021.131890.

23. Elsherif K.M., El-Hashani A., Haider I., 2018. Biosorption of Fe (III) onto Coffee and Tea Powder: Equilibrium and Kinetic Study. Asian J Green Chem. 2(4), 380–394. https://doi .org/10.22034/ ajgc.2018.65163.

24. Elsherif K.M., Ewlad-Ahmed A.M., Treban A., 2017. Removal of Fe (III), Cu (II), and Co (II) from Aqueous Solutions by Orange Peels Powder: Equilibrium Study. World J Biochem Mol Biol. 2(6), 46–51.

25. Meili L., Lins P.V.S., Costa M.T., Almeida R.L., Abud A.K.S., Soletti J.I., Dotto G.L., Tanabe E.H., Sellaoui L., Carvalho S.H.V., Erto A., 2019. Adsorption of Methylene Blue on Agroindustrial Wastes: Experimental Investigation and Phenomenological Modelling. Prog Biophys Mol Biol. 141, 60–71. https://doi.org/10.1016/j.pbiomolbio.2018.07.011.

26. Li H., Budarin V.L., Clark J.H., North M., Wu X., 2022. Rapid and Efficient Adsorption of Methylene Blue Dye from Aqueous Solution by Hierarchically Porous, Activated Starbons®: Mechanism and Porosity Dependence. J Hazard Mater. 436, 129174. https://doi.org/ 10.1016/j.jhazmat.2022.129174.

27. Elsherif K.M., El-Hashani A., El-Dali A., 2013. Potentiometric Determination of Fixed Charge Density and Permselectivity for Silver Thiosulphate Membrane. J Appl Chem. 2(6), 1543–1551.

28. Miyah Y., Lahrichi A., Idrissi M., Khalil A., Zerrouq F., 2018. Adsorption of Methylene Blue Dye from Aqueous Solutions onto Walnut Shells Powder: Equilibrium and Kinetic Studies. Surf Interfaces. 11, 74–81. https://doi.org/10.1016/j.surfin.2018.03.006.

29. Üner O., Geçgel Ü., Bayrak Y., 2016. Adsorption of Methylene Blue by an Efficient Activated Carbon Prepared from Citrullus Lanatus Rind: Kinetic, Isotherm, Thermodynamic, and Mechanism Analysis. Water Air Soil Pollut. 227(7), 247. https://doi.org/10.1007/s11270-016-2949-1.

30. Adesina A.O., Elvis O.A., Mohallem N.D.S., Olusegun S.J., 2021. Adsorption of Methylene Blue and Congo Red from Aqueous Solution Using Synthesized Alumina–Zirconia Composite. Environ Technol. 42(7), 1061-1070. https://doi.org/10. 1080/09593330.2019.1652696.

31. Lelifajri, Rahmi, Supriatno, Susilawati, Indarum A.S.M., 2020. Study on Methylene Blue Dye Adsorption in Aqueous Solution by Heat-Treated Gnetum Gnemon Shell Waste Particles as Low-Cost Adsorbent. AIP Conf. Proc. 2243, 020012. https://doi.org/10.1063/5.0001358.

32. Vargas A.M.M., Cazetta A.L., Kunita M.H., Silva T.L., Almeida V.C., 2011. Adsorption of Methylene Blue on Activated Carbon Produced from Flamboyant Pods (*Delonix Regia*): Study of Adsorption Isotherms and Kinetic Models. Chem Eng J. 168, 722–730. https://doi.org/ 10.1016/j.cej.2011.01.067.

33. Thang N.H., Khang D.S., Hai T.D., Ngac D.T., Tuan P.D., 2021. Methylene Blue Adsorption Mechanism of Activated Carbon Synthesized from

Cashew Nut Shells. RSC Adv. 11, 26563. https://doi.org/10.1039/d1ra04672a.

34. He X., Male K.B., Nesterenko P.N., Brabazon D., Paull B., Luong J.H.T., 2013 Adsorption and Desorption of Methylene Blue on Porous Carbon Monoliths and Nanocrystalline Cellulose. ACS Appl Mater Interfaces. 5, 8796–8804. https://doi.org/10.1021/am403222u.

35. Derakhshan Z., Baghapour M.A., Ranjbar M., Faramarzian M., 2013. Adsorption of Methylene Blue Dye from Aqueous Solutions by Modified Pumice Stone: Kinetics and Equilibrium Studies. Health Scope. 2(3), 136–144. https://doi.org/10.17795/jhealthscope-12492.

36. Gao J.J., Qin Y.B., Zhou T., Cao D.D., Xu P., Hochstetter D., Wang Y.F., 2013 Adsorption of Methylene Blue onto Activated Carbon Produced from Tea (*Camellia Sinensis* L.) Seed Shells: Kinetics, Equilibrium, and Thermodynamics Studies. J Zhejiang Univ Sci. B14(7), 650–658. https://doi.org/10.1631/jzus.B12a0225.

37. Liu Q.X., Zhou Y.R., Wang M., Zhang Q., Ji T., 2019. Adsorption of Methylene Blue from Aqueous Solution onto Viscose-Based Activated Carbon Fiber Felts: Kinetics and Equilibrium Studies. Adsorpt Sci Technol. 37(3-4), 312–332. https://doi.org/10.1177/0263617419827437.

38. El-Shafie A.S., Karamshahi F., El-Azazy M., 2023. Turning Waste Avocado Stones and Montmorillonite into Magnetite-Supported Nanocomposites for the Depollution of Methylene Blue: Adsorbent Reusability and Performance Optimization. Environ Sci Pollut Res. No Pagination Specified. 30, 118764–118781. https://doi.org/10.1007/s11356-023-30538-0.

39. Elashery S.E.A., El-Bouraie M.M., Abdelgawad E.A., Attia N.F., Mohamed G.G., 2023. Adsorptive Performance of Bentonite-Chitosan Nanocomposite as a Dual Antibacterial and Reusable Adsorbent for Reactive Red 195 and Crystal Violet Removal: Kinetic and Thermodynamic Studies. Biomass Convers Biorefin. https://doi.org/10.1007/s13399-023-05059-y.

40. Amode J.O., Santos J.H., Alam Z.M., Mirza A.H., Mei C.C., 2016. Adsorption of Methylene Blue from Aqueous Solution Using Untreated and Treated (Metroxylon Spp.) Waste Adsorbent: Equilibrium and Kinetics Studies. Int J Ind Chem. 7, 333–345. https://doi.org/10.1007/s40090-016-0085-9.

41. Elsherif K.M., Saad R.A.A., Ewlad-Ahmed A.M., Treban A.A., Iqneebir A.M., 2024. Adsorption of Cd(II) onto Olive Stones Powder Biosorbent: Isotherms and Kinetic Studies. Adv. J Chem Sect. A7(1), 59–74. https://doi.org/ 10.48309/ ajca.2024.415865.1415.

42. Alkherraz A.M., Ali A.K. El-Dali A., Elsherif K.M., 2019. Biosorption Study of Zn(II), Cu(II), Pb(II) And Cd(II) Ions by Palm Leaves Activated Carbon. To Chem. 4(2019), 8–17.

43. Elsherif K.M., El-Dali A., Ewlad-Ahmed A.M., Treban A.A., Alqadhi H., Alkarewi S., 2022. Kinetics and Isotherms Studies of Safranin Adsorption onto Two Surfaces Prepared from Orange Peels. Mor J Chem. 10(4), 639–651. https://doi.org/10.48317/IMIST.PRSM/morjchem-v11i1.32137.

44. El-Bery H.M., Saleh M., El-Gendy R.A., Saleh M.R., Thabet S.M., 2022. High Adsorption Capacity of Phenol and Methylene Blue Using Activated Carbon Derived from Lignocellulosic Agriculture Wastes. Sci Rep. 12(1), 5499. https://doi.org/10.1038/s41598-022-09475-4.

45. Elsherif K.M., Haider I., El-Hashani A., 2019. Adsorption of Co (II) Ions from Aqueous Solution onto Tea and Coffee Powder: Equilibrium and Kinetic Studies. J Fundam Appl Sci. 11(1), 65–81. https://doi.org/10.4314/jfas.v11i1.5.

46. Elsherif K.M., El-Hashani A., Haider I., 2018. Equilibrium and Kinetic Studies of Cu (II) Biosorption Onto Waste Tea and Coffee Powder (WTCP). Iran J Anal Chem. 5(2), 31–38. https://doi.org/20.1001.1.23832207.2018.5.2.5.4.

47. El-Hashani A., Elsherif K.M., Edbey K., Alfaqih F., Alomammy M., Alomammy S., 2018. Biosorption of Eriochrome Black T (EBT) onto Waste Tea Powder: Equilibrium and Kinetic Studies. To Chem. 1(3), 263–275.

48. Elsherif K.M., El-Dali A., Ewlad-Ahmed A.M., Treban A., Alttayib I., 2021. Removal of Safranin Dye from Aqueous Solution by Adsorption onto

Olive Leaves Powder. J Mater Environ Sci. 12(3), 418–430.

49. Mohamed F., Shaban M., Zaki S.K., Abd-Elsamie M.S., Sayed R., Zayed M., Khalid N., Saad S., Omar S., Ahmed A.M., Gerges A., Abd El-Mageed H.R., Soliman N.K., 2022. Activated Carbon Derived from Sugarcane and Modified with Natural Zeolite for Efficient Adsorption of Methylene Blue Dye: Experimentally and Theoretically Approaches. Sci Rep. 12(18031). https://doi.org/10.1038/s41598-022-22421-8.

50. Fito J., Abewaa M., Mengistu A., Angassa K., Ambaye A.D., Moyo W., Nkambule T., 2023. Adsorption of Methylene Blue from Textile Industrial Wastewater Using Activated Carbon Developed from Rumex Abyssinicus Plant. Sci Rep. 13, 5427. https://doi.org/10.1038/s41598-023-32341-w.

51. Alardhi S.M., Salih H.G., Ali N.S., Khalbas A.H., Salih I.K., Cata Saady N.M., Zendehboudi S., Albayati T.M., Harharah H.N., 2023. Olive Stone as an Eco-Friendly Bio-Adsorbent for Elimination of Methylene Blue Dye from Industrial Wastewater. Sci Rep. 13, 21063. https://doi.org/10.1038/s41598-023-47319-x.

52. Modi S., Yadav V.K., Ali D., Choudhary N., Alarifi S., Sahoo D.K., Patel A., Fulekar M.H., 2023. Photocatalytic Degradation of Methylene Blue from Aqueous Solutions by Using Nano-ZnO/Kaolin-Clay-Based Nanocomposite. Water. 15(22), 3915. https://doi.org/10.3390/w15223915.

53. Turp S.M., Turp G.A., Ekinci N., Özdemir S., 2020. Enhanced Adsorption of Methylene Blue from Textile Wastewater by Using Natural and Artificial Zeolite. Water Sci. Technol. 82(3), 513–523. https://doi.org/10.2166/wst.2020.358.

54. Wang G., Wang S., Sun Z., Zheng S., Xi Y., 2017. Structures of Nonionic Surfactant Modified Montmorillonites and Their Enhanced Adsorption Capacities towards a Cationic Organic Dye. Appl Clay Sci. 148, 1–10. https://doi.org/10.1016/j.clay.2017.08.001.

55. Santoso E., Ediati R., Kusumawati Y., Bahruji H., Sulistiono D.O., Prasetyoko D., 2020. Review on Recent Advances of Carbon Based Adsorbent for Methylene Blue Removal from Waste Water. Mater Today Chem. 16, 100233. https://doi.org /10.1016/j.mtchem.2019.100233.

56. Zhang J., Zhou Q., Ou L., 2012. Kinetic, Isotherm, and Thermodynamic Studies of the Adsorption of Methyl Orange from Aqueous Solution by Chitosan/Alumina Composite. J Chem Eng Data. 57(2), 412–419. https://doi.org/10.1021/je2009945.

57. Vairavel P., Rampal N., Jeppu G., 2023. Adsorption of Toxic Congo Red Dye from Aqueous Solution Using Untreated Coffee Husks: Kinetics, Equilibrium, Thermodynamics and Desorption Study. Int J Environ Anal Chem. 103(12), 2789-2808. https://doi.org/ 10.1080/ 03067319. 2021.1897982.

58. Lafi R., Montasser I., Hafiane A., 2019. Adsorption of Congo Red Dye from Aqueous Solutions by Prepared Activated Carbon with Oxygen-Containing Functional Groups and Its Regeneration. Adsorpt Sci Technol. 37(1–2), 160–181. https://doi.org/10.1177/0263617418819227.

59. Djilani C., Zaghdoudi R., Djazi F., Bouchekima B., Lallam A., Modarressi A., Rogalski M., 2015. Adsorption of Dyes on Activated Carbon Prepared from Apricot Stones and Commercial Activated Carbon. J Taiwan Inst Chem Eng. 53, 112–121. https://doi.org/10.1016/j.jtice.2015.02.025.